# HOHOHO: intracranial HemOrrHage detectiOn enHenced by asymmetric lOss with CNN-LSTM

**Ming-Yang Ho**
何明洋
r08945027
Graduate Institute of Biomedical Engineering and Bioinformatics
r08945027@ntu.edu.tw

**Bin-Ray Wu**
吳彬睿
r08942087
Graduate Institute of Communication Engineering
r08942087@ntu.edu.tw

**Hsin-Yu Ho**
何欣育
r08946005
Data Science Degree Program
r08946005@ntu.edu.tw

**Si-Yang Jiang**
蔣思陽
r08921098
Graduate Institute of Electrical Engineering
r08921098@ntu.edu.tw

## 1 Introduction

Cerebral hemorrhage, bleeding that occurs around or within the brain, is a serious health problem requiring rapid and often intensive medical treatment. The cerebral hemorrhage can be divided into 5 categories: Intracerebral hemorrhage (ICH), Intraventricular hemorrhage (IVH), Subarachnoid hemorrhage (SAH), Subdural hemorrhage (SDH), and Epidural hemorrhage (EDH). While the diagnosis requires an urgent procedure, the process is complicated and often time-consuming. Herein, this problem is attempted to be solved by learning-based methods.

## 2 Methodology or Model Architecture

### 2.1 Preprocessing

Each CT image was firstly stacked with two aside ones in the preprocessing step to extract more information owing to the property of sequential CT scanning (**Figure 3 in appendix**). Limited augmentation strategies, rotation with little color adjustment, were utilized to avoid interfering with the intrinsic CT data distribution.

### 2.2 Models

#### 2.2.1 Big Dataset: CNN-LSTM

ResNet18 was utilized as the features extraction backbone trained with asymmetric loss. Warmup steps were leveraged to avoid unstable model initialization during the previous training, and cosine-annealing learning rate scheduling was applied, which let the model have a chance to jump out if it got stuck into a local minimum.

Finally, a stacked LSTM architecture trained with BCE loss, utilizing 512-dim embedding from ResNet18, was leveraged to further enhance the overall performance. The main effect of the LSTM model is to get the temporal information, which thoroughly considers a patient at the same time. Shortcuts were made from every stage of LSTM output and then add to the final FC layer, which

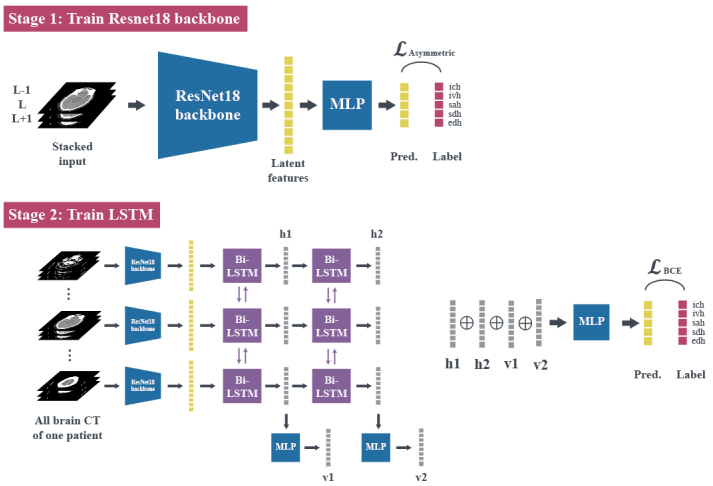


Figure 1: **CNN-LSTM:** ResNet18 backbone, with layer shortcut Bi-LSTM.

could solve the gradient vanishing problems and make training converged faster **(Figure 4 in appendix)**.

#### 2.2.2 Small Dataset: Self-supervised Learning with Backbone

SimCLR[1] is a method that uses data augmentations for distinguishing features in the latent space. Specifically, after the feature extractor, the contrast loss is defined, which helps the positive features become more closely and the negative ones more farther away from each other. Due to the label deficiency in the small dataset, this technique, which enables distinguishing the positive and negative samples without labels via appropriate data augmentations, was utilized to overcome this problem. Afterward, the pretrained weight from SimCLR was fine-tuned by the labels from the small dataset **(Figure 1)**.

### 2.3 Loss functions

**Asymmetric Multi-label Loss (stage-1)**

$$\begin{cases} \mathcal{L}_+ = (1-p)^{\gamma_+}\log(p), \\ \mathcal{L}_- = p^{\gamma_-}\log(1-p). \end{cases} \tag{1}$$

Asymmetric loss[2], an improved focal loss designed for unbalanced positive and negative samples training with a tunable parameter $\gamma$ controlling the model to focus on positive samples, was utilized. It was found that the positive and negative portion of the dataset was 13:1, so $\gamma_+ = 0$ and $\gamma_- = 2$ were chosen. Furthermore, a clip design, which would prune the class if the confidence of the class was extremely excessive, would enable those uncertain classes to have more possibilities to be trained and allow the model to get their features.

## 3 Implementation Details

### 3.1 Hyperparameter Choices during preprocessing

All the CT images were stacked into three channels. Random rotate(40), random horizontal flip and random color jitter (brightness=0.1, contrast=0.1, saturation=0.1, hue=0) with apply probability=0.4

strategies were selected for augmentation while in the valid setting, images were simply transformed into tensor.

### 3.2 Hyperparameter Choices during model training

Regarding the full dataset training, cosine-annealing learning rate scheduling was set from $2 \times 10^{-4}$ to $10^{-5}$ with Adam optimizer, and batch size was set to 48. During the LSTM training stage, the LSTM unit was set at 64 with batch size at a value of 32. For the small dataset, ResNet18 was also selected as the backbone. BCE loss with pos_weight and Adam were used as loss function and optimizer, respectively. The learning rate was set at $10^{-3}$ and the batch size was 48. During the SimCLR, 0.5 was selected as the temperature parameter.

## 4 Experiments

### 4.1 Results

| | | ResNet 18 (rotation 20) | | ResNet 18 (rotation 40) | |
|---|---|---|---|---|---|
| Batch size | | 4 | 64 | 64 | 128 |
| LSTM units | | 64 | 64 | 64 | 64 |
| Stacked | Train f2 | 0.8907 | 0.8943 | 0.8957 | 0.8988 |
| | Val f2 | 0.7714 | 0.7714 | 0.7917 | 0.7911 |
| | Test f2 | 0.7792 | 0.7787 | 0.7764 | 0.7726 |

Table 1: Comparison results of stage 2 LSTM with different rotation angles

| Dataset | | Full | Small |
|---|---|---|---|
| Best | Train f2 | 0.8907 | 0.6928 |
| | Val f2 | 0.7714 | 0.5971 |
| | Test f2 | 0.7792 | 0.6450 |

Table 2: Best results

For the case of using a full training dataset, multitudinous optimizers and augmentation parameters were firstly investigated with vanilla ResNet18 trained with BCE loss, which demonstrated the detrimental effect of either large batch size or color adjustment. However, the model with BCE loss could only achieve at most 73.10% f2 score **(Table 3 in appendix)**. If BCE loss was replaced with asymmetric loss, the model could achieve 2.50% f2 enhancement, compared to the former one. It showed that asymmetric loss is an effective strategy to further improve model performance **(Table 6 in appendix)**. Moreover, two-stage training with stacked LSTM, which had been introduced in chapter 3, obtained the best performance with 78.25%. Comparing to the ResNet18 model which trained with asymmetric loss, it enabled approximate 2.75% f2 enhancement **(Table 1 and 2)**. As for the case of using small a training dataset, the self-supervised model obtained the best performance with 64.50% **(Table 2)**.

Besides the designs of model architecture, multifarious strategies were also leveraged, struggling to find a better performance. However, the endeavor was in vain **(Table 4 and 5 in appendix)**.

### 4.2 T-SNE

According to the close observation of raw CT data, it was found that all patients were scanned from the vertex to different endpoints, such as at mandibular and ocular level. It led to the fact that not every patient had the same number of images.

To visualize and analyze the latent space of the ResNet18 backbone model, the t-SNE technique was utilized. Embeddings of images were firstly extracted from different datasets and then reduced from 512 dimensions to 2 dimensions. Considering the original rules of position labeling, which labeled

vertex to mandibular as 0 to 45, all the position levels were accordingly reversed for each patient (i.e. 0 denotes the vertex). It showed that the embeddings of vertex CT images and mandibular CT images were clustering together on the left side of the three t-SNE plots while the embeddings of middle CT images were on the right side. Therefore, it could be claimed that our ResNet18 backbone model could learn the position information, and position information was not required to be provided as an additional feature for training **(Figure 2)**.

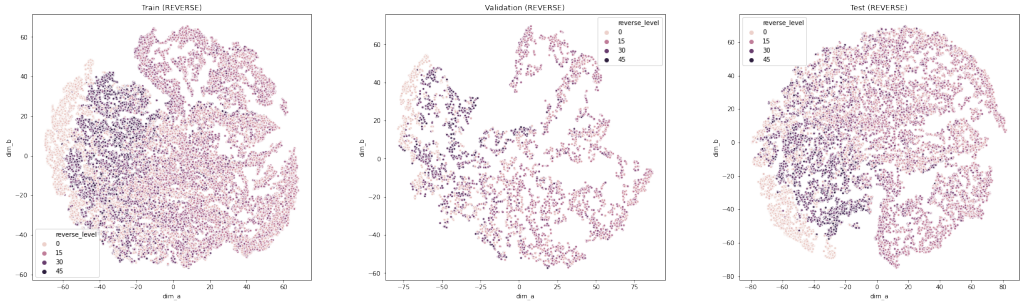


(a) Training dataset (b) Validation dataset (c) Testing dataset

Figure 2: t-SNE for embeddings extracted by ResNet18 backbone model.

### 4.3 Saliency map

To elucidate what did the model learn, an explainable saliency map was further utilized **(Figure 5 in appendix)**. The left pair unequivocally showed that the model did focus on the region where the ICH occurred. On the other hand, the saliency region distributed somehow evenly in the right pair, which, thus, was predicted erroneously.

### 4.4 Mislabeled

Some strange patterns, for example, "...101..." and "10101", did exist in the provided ground-true labels. After a thorough examination, several of them were mislabeled and would deteriorate the model performance **(Figure 6 in appendix)**. However, our model could still predict the diagnosis correctly, which definitely demonstrates the advantages of deep learning model utilization in the clinical scenario to reduce misdiagnosis.

## 5 Conclusion

The merit of utilizing stacked CT images, novel asymmetric loss, and Bi-LSTM to enhance the vanilla CNN model in ICH multi-label prediction is demonstrated in this work. Some unreasonable data augmentation or training strategies that would deteriorate model performance are also explicated in the aforementioned experiments. Besides, explainable saliency maps and distribution of embedding space enable insight into what the model learned. Finally, the correct prediction of erroneously labeled data does manifest the unprecedented potential of leveraging deep learning technique in the clinical diagnosis assistance.

## References

[1] Chen, T. & Kornblith, S., Norouzi, M. & Hinton, G. (2020) A simple framework for contrastive learning of visual representations. *arXiv preprint arXiv:2002.05709*

[2] Ben-Baruch, E. & Ridnik, T. & Zamir, N. & Noy, A., Friedman, I. & Protter, M. & Zelnik-Manor, L. (2020). Asymmetric Loss For Multi-Label Classification. *arXiv preprint arXiv:2009.14119*

# 6 Appendix

**Focal Loss**

$$\begin{cases} \mathcal{L}_{+} = (1-p)^{\gamma}\log(p), \\ \mathcal{L}_{-} = p^{\gamma}\log(1-p). \end{cases} \tag{2}$$

**Binary Cross Entropy Loss (stage-2)**

$$\mathcal{L} = p\,\log(p) + (1-p)\log(1-p) \tag{3}$$

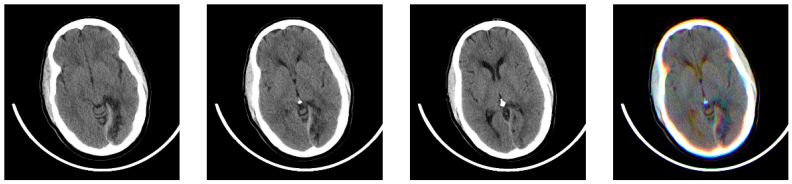

(a) *l-1* (b) *l* (c) *l+1* (d) *3 Channels*

Figure 3: (a)(b)(c) are CT images. For a training sample, we stacked 3 consecutive CT images.

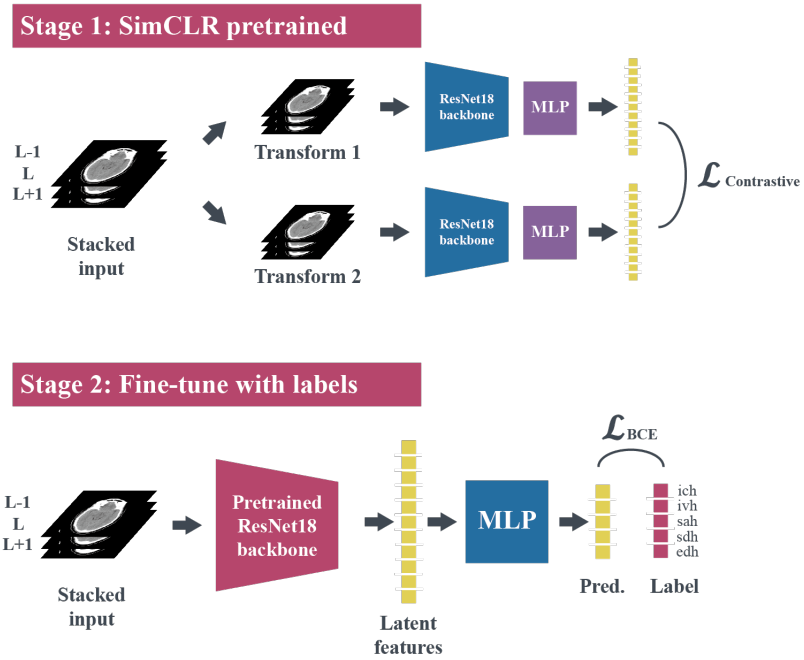


Figure 4: **SimCLR:** ResNet18 backbone, with SimCLR pre-trained

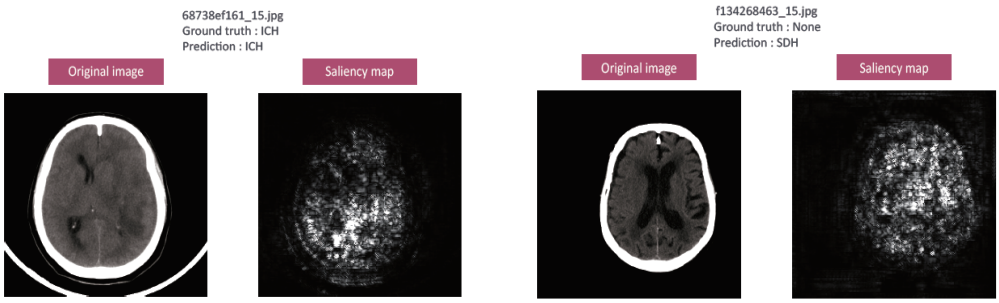


(a) Match (b) Mismatch

Figure 5: Saliency map examples

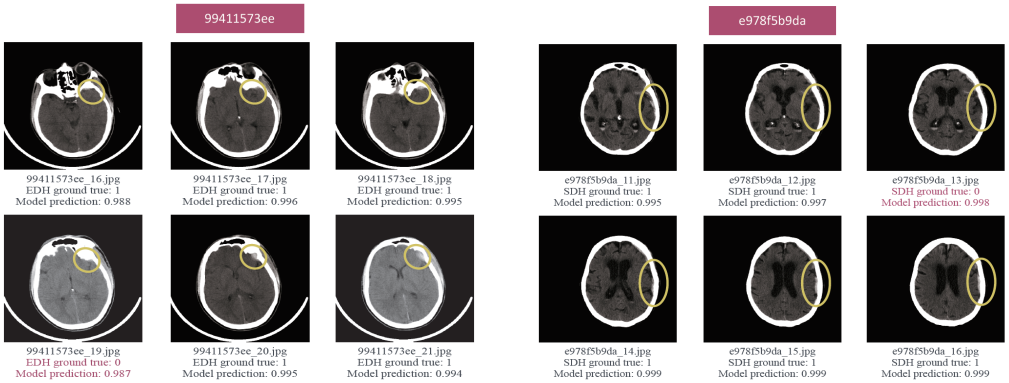


(a) Case 1 (b) Case 2

Figure 6: Mislabeled examples

| | | Adam | | SGD | | | SGD No nesterov |
|---|---|---|---|---|---|---|---|
| Batch size | | 64 | 40 | 64 | 40 | | 40 |
| Colorjitter | | 0.5 | 0.1 | 0.1 | 0.2 | | 0.1 |
| Rotation | | 20 | 20 | 20 | 30 | 30 | 30 |
| Gray | Train f2 | 0.8496 | 0.7273 | 0.8612 | 0.8140 | 0.7480 | - |
| | Val f2 | 0.6892 | 0.7045 | 0.7064 | 0.7143 | 0.7155 | - |
| Stacked | Train f2 | 0.7208 | 0.7986 | 0.8140 | 0.8408 | 0.7726 | 0.7377 |
| | Val f2 | 0.7011 | 0.7000 | 0.7143 | 0.7307* | 0.7175 | 0.7153 |

Table 3: Comparison results of vanilla ResNet18 under different hyperparameters settings

| Attempt | | ResNet-34 With Adam BCE Loss | ResNet-34 With SGD BCE Loss | ResNet-50 With Adam BCE Loss | ResNet-50 With SGD BCE Loss | DenseNet121 With Adam BCE Loss | DenseNet121 With Adam BCE Loss |
|---|---|---|---|---|---|---|---|
| Stacked | Train f2 | 0.870 | 0.979 | 0.687 | 0.832 | 0.818 | 0.796 |
| | Val f2 | 0.637 | 0.647 | 0.637 | 0.712 | 0.731 | 0.730 |
| | Test f2 | 0.717 | 0.708 | 0.698 | 0.716 | 0.735 | 0.734 |

Table 4: Other attempts with vanilla ResNet and DenseNet

| Attempt | | ResNet-18 Asymmetric Loss Relabeled with 0.5 | ResNet-18 Asymmetric Loss Relabeled with 1 | ResNet-18 Asymmetric Loss Filtered data | ResNet-18 Asymmetric Loss Magic normalization | CNN-LSTM END2END |
|---|---|---|---|---|---|---|
| Stacked | Train f2 | 0.812 | - | 0.881 | 0.848 | 0.824 |
| | Val f2 | 0.757 | 0.769 | 0.753 | 0.759 | 0.741 |
| | Test f2 | 0.700 | 0.744 | 0.727 | 0.743 | - |

Table 5: Other attempts with multifarious tricks

| | | Adam with asymmetric loss | | | | | |
|---|---|---|---|---|---|---|---|
| Colorjitter | | 0 | 0.1 | 0.2 | 0.1 | 0.1 | 0.1 |
| Rotation | | 20 | 20 | 20 | 30 | 40 | 50 |
| Stacked | Train f2 | 0.843 | 0.842 | 0.829 | 0.865 | 0.843 | 0.854 |
| | Val f2 | 0.741 | 0.743 | 0.729 | 0.781 | 0.773 | 0.771 |
| | Test f2 | 0.743 | 0.750 | 0.735 | 0.736 | 0.749 | 0.755 |

Table 6: Comparison results of ResNet18 with asymmetric loss under different hyperparameters settings